Use of Support Vector Regression in Stable Trajectory Generation for Walking Humanoid Robots

Dong Won Kim, Sam-Jun Seo, Clarence W. de Silva, Gwi-Tae Park

This paper concerns the use of support vector regression (SVR), which is based on the kernel method for learning from examples, in identification of walking robots. To handle complex dynamics in humanoid robot and realize stable walking, this paper develops and implements two types of reference natural motions for a humanoid, namely, walking trajectories on a flat floor and on an ascending slope. Next, SVR is applied to model stable walking motions by considering these actual motions. Three kinds of kernels, namely, linear, polynomial, and radial basis function (RBF), are considered, and the results from these kernels are compared and evaluated. The results show that the SVR approach works well, and SVR with the RBF kernel function provides the best performance. Plus, it can be effectively applied to model and control a practical biped walking robot.

Keywords: SVM, zero moment point, walking pattern identification, stability of humanoid robots.

Manuscript received Aug. 13, 2008; revised June 19, 2009; accepted Aug. 18, 2009.

This work was supported by the Korea Research Foundation Grant funded by the Korean Government (MOEHRD, Basic Research Promotion Fund) (KRF-2008-521-D00137).

Dong Won Kim (phone: +82 32 870 2215, email: dwnkim@inhatc.ac.kr) was with the Department of Electrical Engineering and Computer Sciences, University of California, Berkeley, CA, USA, and is now with the Department of Digital Electronics, Inha Technical College, Incheon, Rep. of Korea.

Sam-Jun Seo (email: ssj@anyang.ac.kr) is with the Department of Electrical and Electronic Engineering, Anyang University, Gyeonggido, Rep. of Korea.

Clarence W. de Silva (email: desilva@mech.ubc.ca) is with the Department of Mechanical Engineering, University of British Columbia, Vancouver, Canada.

Gwi-Tae Park (email: gtpark@korea.ac.kr) is with the Department of Electrical Engineering, Korea University, Seoul, Rep. of Korea.

doi:10.4218/etrij.09.0108.0452

I. Introduction

Humanoid robots–human-shaped and human-like walking robots–are thought to have better mobility for locomotion and dexterity of manipulation than conventional mobile robots. Humanoid robots can be used as proxies or service providers for humans, performing tasks in real world environments, including rough terrain, steep stairs, and obstacles, both static and dynamic. This is the primary motive for the development of humanoid robots [1]. Humanoid robots have recently evolved into an active area of research and development, with the creation of several humanoid robot systems. Many related issues such as stability criteria, robot design and development, and dynamics analysis have been studied [2]-[5], and many technical issues have to be resolved. Among these issues, stable and reliable biped walking is a fundamental issue that has yet to be resolved with a high degree of reliability. To realize human-like walking robots, many studies on biped robot locomotion and theories of bipedal walking have been carried out. In [6], six theories of bipedal walking are considered and supporting evidence for these theories is explored. In [7], the basic rhythm underlying animal locomotion is created by dedicated neural structures called central pattern generators, and the implementation of such structures in simulation and their successful use for the control of bipedal walking are described. To emulate the actual neuro-control mechanism of human bipedal locomotion, an anatomy- and physiology-based neuro-muscular-skeletal model is developed in [8]. A real-time joint trajectory generator for planar walking bipeds is proposed in [9]. In [10], a hierarchical evolutionary algorithm is proposed to generate a walking motion through energy optimization and to generate a natural motion by considering the zero moment point (ZMP). Current research is directed

toward the generation of anthropomorphic trajectories, and toward the development of efficient ways for the biped robot to control them.

Vukobratovic and others [11] investigated walking dynamics and proposed ZMP as an index of walking stability. Shih [12], Dasgupta [13], Takanishi [14], and Hirai [15] have proposed methods for walking pattern synthesis based on the ZMP, and demonstrated walking motion using real robots. The ZMP, which is defined as the point on the ground about which the sum of all the moments of the active forces equals zero, is indispensable in ensuring the dynamic stability of a biped robot. If the ZMP is within the convex hull of all contact points between the feet and ground, the biped robot is able to walk. This convex hull of all contact points is known as the stable region [16]. As a result, ZMP trajectories are used as a reference for stable walking by humanoid robots. Recently, researchers have attempted to develop human-like walking by modeling the desired ZMP trajectory. In previous studies [17]-[19] we employed a fuzzy system and a neuro-fuzzy technique to generate a smooth walking pattern, and our results were known to be original and unconventional. This stems mainly from the relatively higher predictive ability of fuzzy systems than their statistical regression counterparts [18]. However, other intelligent approaches like the method of support vector regression (SVR) have not yet been evaluated. The applicability of SVR to humanoid robots needs be investigated since it may provide better predictions than typical fuzzy systems and thereby provide better insight into human-like walking mechanisms.

In this study, SVR is applied to model the ZMP trajectory of a practical humanoid robot. The performance of SVR can vary considerably depending on the type of kernels adopted by the networks. In this paper, the performance is optimized as a function of three kinds of kernels: linear, polynomial, and radial basis function (RBF). The SVR model is compared with the fuzzy system, neuro-fuzzy system, and classical statistical regression models.

II. Prototype Biped Humanoid Robot

The practical biped humanoid robot shown in Fig. 1(a) has been designed and implemented in this study. The robot has 19 joints, and their arrangement during motion is shown in Fig. 1(b). The height and the total weight are 380 mm and 2700 g, including the batteries and the CCD camera mounted on the robot body, respectively. Each joint is driven by a radio controlled (RC) servomotor, which consists of a DC motor, gear, and a simple controller. Each RC servomotor is mounted on the link structure. The specifications of our humanoid robot are given in Table 1.

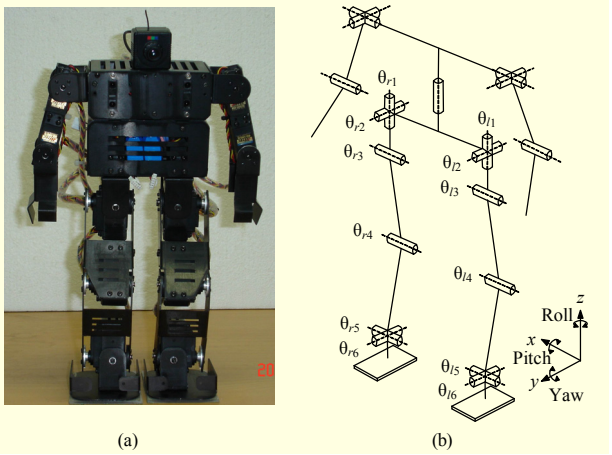

Fig. 1. (a) Prototype humanoid robot and (b) its joint structure and angle representation.

Table 1. Specifications of the prototype humanoid robot.

Height	380 mm
Weight	2700 g
CPU	TMS320LF2407 DSP
Actuator (RC servo motors)	HSR-5995TG (torque: 30 kg·cm at 7.4 V)
Degree of freedom	19 DOF (leg+arm+waist) = 2×6 + 3×2+1
Power source (Battery)	Actuator: AA size Ni-poly (7.4 V, 1700 mAh)
	Control board: AAA size Ni-poly (7.4 V, 700 mAh)

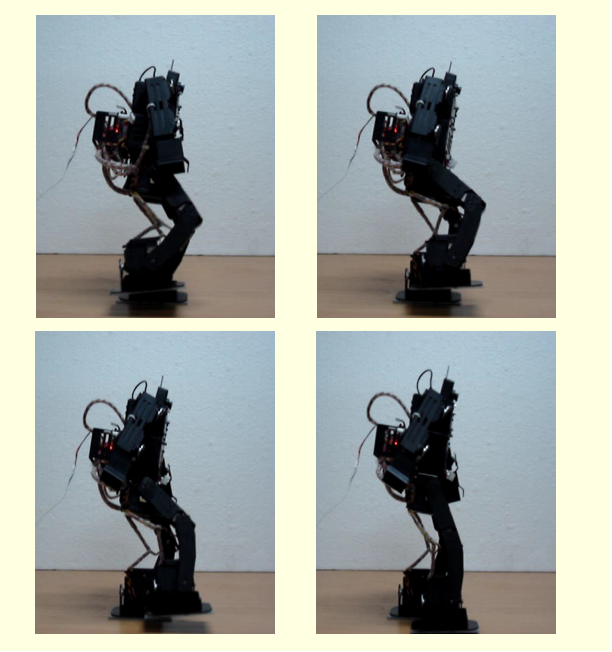

Fig. 2. Biped humanoid robot walking on a flat floor.

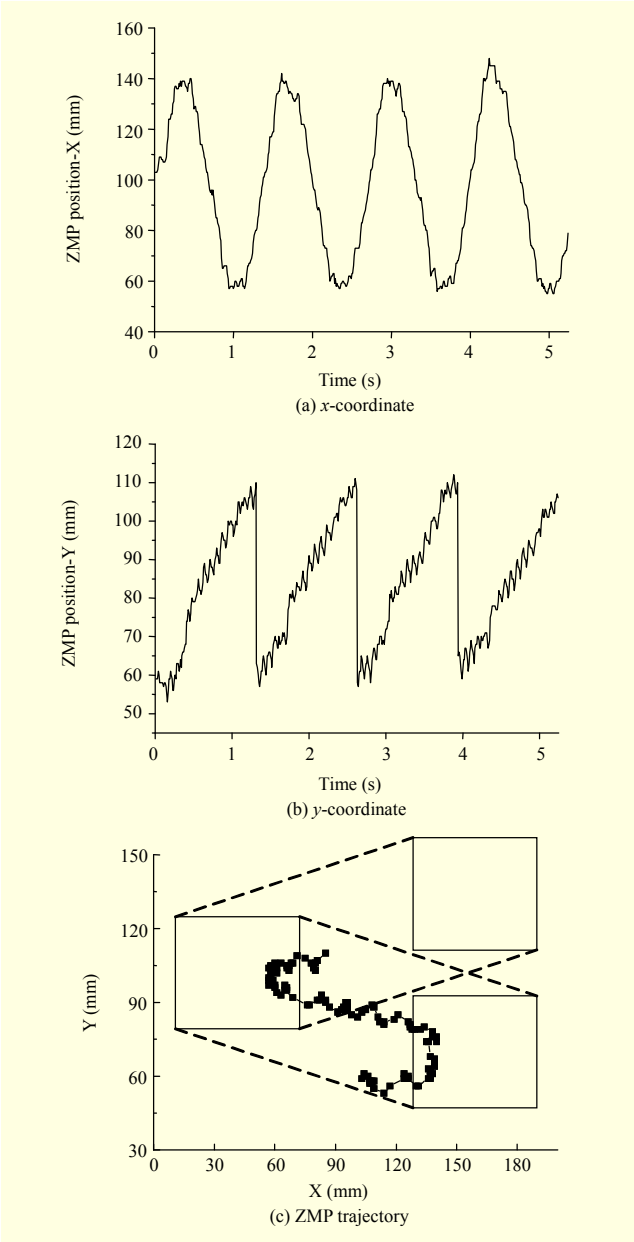

Fig. 3. Ideal ZMP positions and corresponding trajectory of a biped humanoid robot.

The ZMP trajectory is used as a stability criterion, and the real ZMP is computed based on the data given by the force sensors on each foot. The walking motions of the robot on a flat surface are shown in Fig. 2. The ideal ZMP positions, *x*-coordinate and *y*-coordinate, and their corresponding ZMP trajectories from [18] are also shown in Fig. 3.

During a walking cycle, there are two phases: the statically stable double-support phase, when the robot is supported on both feet simultaneously, and the statically unstable single-support phase, when only one foot of the robot is in contact with the ground while the other is being transferred from the back to front positions. Thus, the locomotion of the robot changes its structure during a single walking cycle. In the ZMP trajectories shown in Fig. 3(c), the rectangular symbol denotes the foot, and the ZMP positions of the humanoid walking robot are in each foot during the single support phases. To ensure dynamic stability of the humanoid robot, ZMP must exist in each foot. Meanwhile, the hexagonal symbol denotes the double support phase, and the ZMP must exist in this domain as well. The trajectory of biped humanoid robot shown in Fig. 3(c) indicates that all the positions of ZMP are in the domain of the stable region; therefore, the humanoid walking robot is stable.

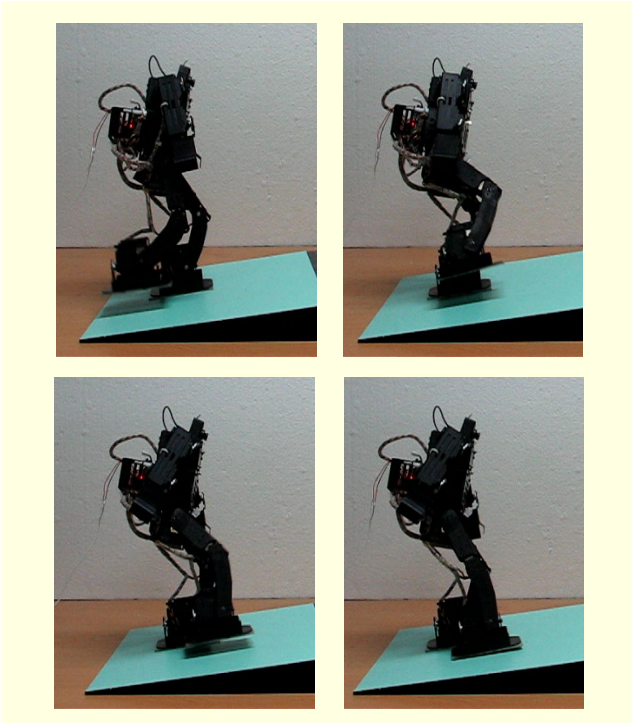

Fig. 4. Biped humanoid robot walking up a slope.

Figure 4 depicts the walking motion of the humanoid robot when it is walking up an inclined surface. In addition, Fig. 5 shows the ideal ZMP positions and their corresponding trajectories.

The joint locations during walking are shown in Fig. 6. The ideal ZMP trajectory data is obtained from 10 degrees of freedom (DOFs) as shown in Fig. 6. A total of 5 DOFs are assigned to each leg; two are assigned to the hip, two to the ankle, and one to the knee. The cyclic walking pattern has been realized from these joint angles. Our biped walking robot can walk continuously without falling down. Joint angles in the four step motion of our humanoid robot are shown in Fig. 7. Support vector regression, as presented in the next section, is applied to model the ZMP trajectory of the humanoid robot. The performance of SVR is optimized with a variety of kernel

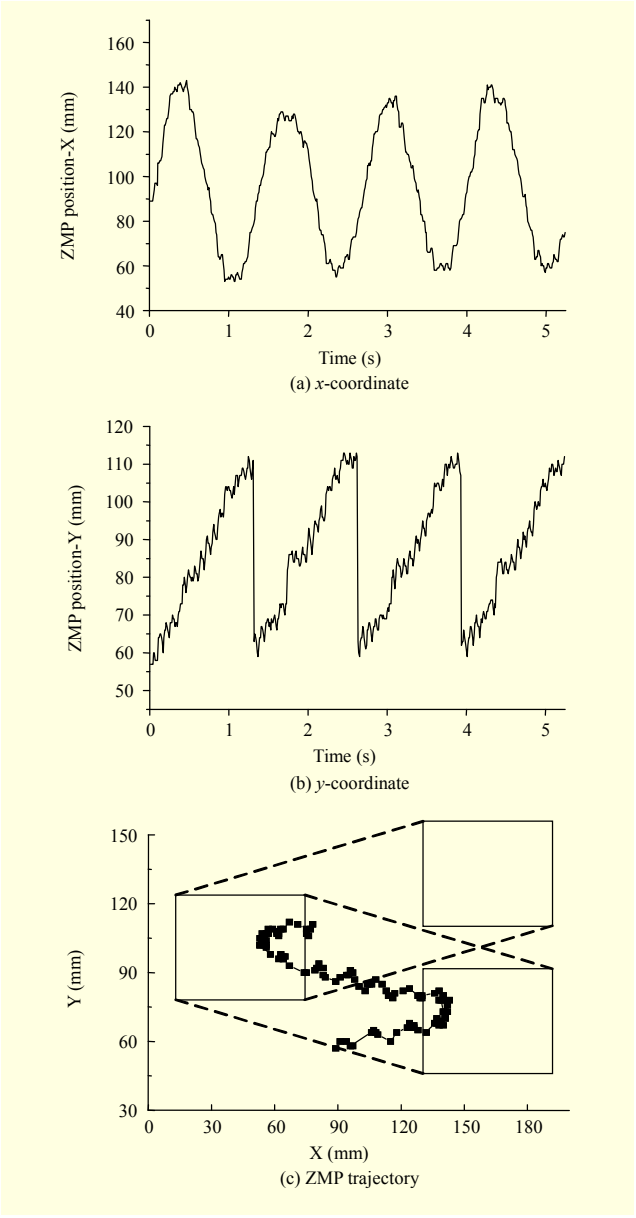

Fig. 5. Ideal ZMP positions and corresponding trajectory of biped humanoid robot.

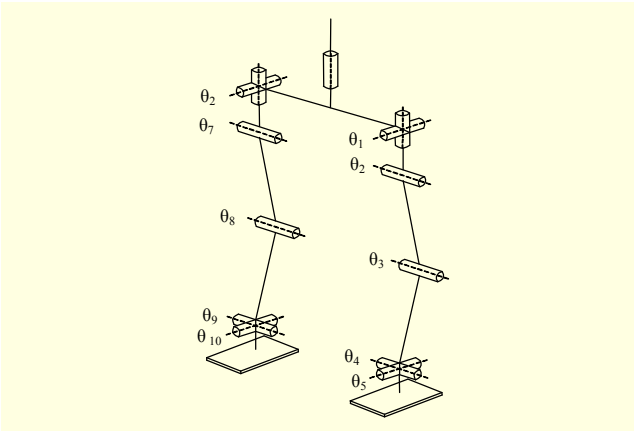

Fig. 6. Joint angle representation of the 10 degrees of freedom.

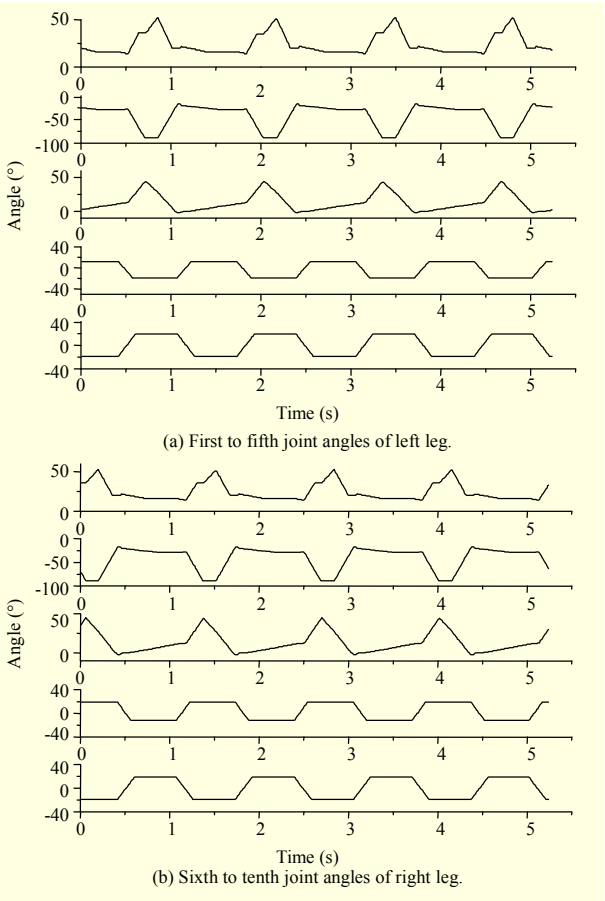

Fig. 7. Joint angles of the humanoid robot depicted in Fig. 6.

functions. The measured data from the 10 DOFs is shown in Fig. 7, and is used as process parameters, input data for ZMP trajectories, and output data.

The ZMP trajectory in the robot foot support area is a significant criterion for the stability of the walk. The ZMP concept has been properly comprehended by researchers, widely used, and frequently cited. Its interpretation is summarized below. Further discussion on the ZMP concept and conditions is found in [10], [20]. Figure 8 shows the concepts of ZMP and stability margin, where p is the point at which $T_x = 0$, $T_y = 0$, and T_x and T_y represent the moments around the x-axis and y-axis generated by the reaction force F_r and the reaction torque T_r, respectively. Point P is defined as the ZMP.

When ZMP exists within the domain of the support surface, the contact between the ground and the support leg is stable:

$$P_{ZMP} = (x_{ZMP}, y_{ZMP}, 0) \in S,$$

where P_{ZMP} denotes a position of ZMP, and S denotes a domain

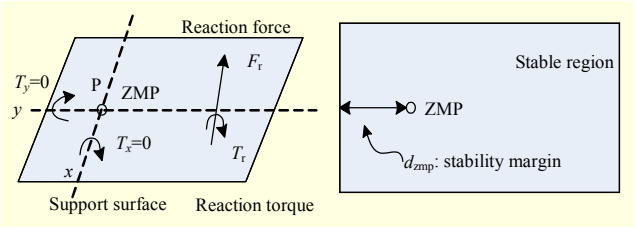

Fig. 8. Concept of ZMP and stability margin.

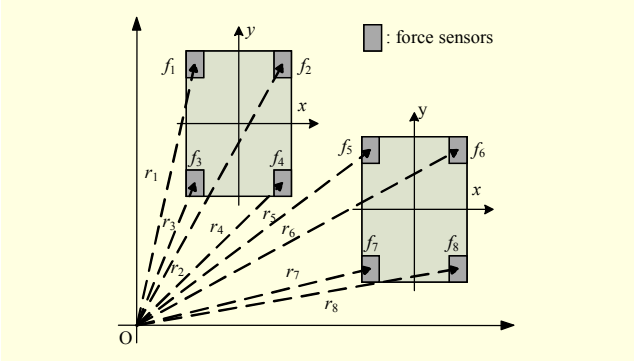

Fig. 9. Distribution of force sensors on the feet.

of the support surface. This condition indicates that no rotation around the edges of the foot occurs.

If the ZMP is within the convex hull of all contact points (the stable region), the biped robot is able to walk. If the minimum distance between the ZMP and the boundary of the stable region is large, the moment preventing the biped robot from tipping over is large as well. The minimum distance d_{zmp} between the ZMP and the boundary of the stable region is called the stability margin [16].

In many studies, ZMP coordinates are computed using a model of the robot and information from the joint encoders. However, in this paper, a more direct approach is employed, which uses measurement data from sensors mounted on the soles of the robot's feet. Figure 9 illustrates the disposition of force sensors on the left and right feet. The type of force sensor used in our experiments is the FlexiForce sensor A201. They are attached to the four corners of the sole plates and measurements are carried out in real time. The foot pressure is obtained by summing the force signals. By using the force sensor data, it is easy to calculate the actual ZMP data. Foot support phase ZMPs in the local foot coordinate frame are computed by

$$P = \frac{\sum_{i=1}^{8} f_i r_i}{\sum_{i=1}^{8} f_i}, \tag{1}$$

where f_i is a force applied to the right and left foot sensors, and r_i is a sensor position, which form vectors. These are also defined in Fig. 9. In the figure, O is the origin of the foot coordinate frame.

III. Support Vector Regression for Stable Walking Patterns

This section presents some basic concepts of the support vector machines (SVM). A more detailed explanation can be found in [21]-[24].

Let $(\mathbf{x}^k, y_k)$, k=1,⋯, m, represent the training examples for the classification problem. Each vector $\mathbf{x}^k \in R^n$ belongs to the class $y_k \in \{-1,+1\}$. Assuming linearly separable classes, there is a separating hyperplane such that

$$y_k(\mathbf{w}^T\mathbf{x}^k + b) > 0, \quad k=1,\cdots,m. \tag{2}$$

The distance between the separating hyperplane and the closest data points is the margin of separation. The goal of an SVM is to maximize this margin. The weights $\mathbf{w}$ and the bias b may be rescaled so that the constraints (2) can be rewritten as

$$y_k(\mathbf{w}^T\mathbf{x}^k + b) \geq 1, \quad k=1,\cdots,m. \tag{3}$$

As a consequence, the margin of separation is $1/\|\mathbf{w}\|$, and the maximization of the margin is equivalent to the minimization of the Euclidean norm of the weight vector. The corresponding weights and bias represent the separating optimal hyperplane. The data point $\mathbf{x}^k$ for which the constraints (3) are satisfied with the equality sign are called support vectors. Introducing the Lagrange multipliers $\alpha_1,\cdots,\alpha_m$, the minimization of $\|\mathbf{w}\|^2$ under constraints (3) can be recast as in [25] in the following dual form:

Find the minimum of

$$J(\boldsymbol{\alpha}) = -\sum_{k=1}^{m}\alpha_k + \frac{1}{2}\sum_{k=1}^{m}\sum_{j=1}^{m}\alpha_k\alpha_j y_k y_j (\mathbf{x}^k)^T\mathbf{x}^j, \tag{4}$$

subject to the linear constraints

$$\sum_{k=1}^{m}\alpha_k y_k = 0, \tag{5}$$

$$\alpha_k \geq 0, \quad k=1,\cdots,m. \tag{6}$$

By solving this QP problem, the optimum Lagrange multipliers α_k are obtained, one for each data point. Using these Lagrange multipliers, the optimum weight vector is determined as

$$\mathbf{w} = \sum_{k=1}^{m}\alpha_k y_k \mathbf{x}^k. \tag{7}$$

Only the Lagrange multipliers corresponding to the support vectors are greater than zero; consequently, the optimum

weights depend uniquely on the support vectors (SVs). For an SV $\mathbf{x}^i$, the optimal hyperplane is $\mathbf{w}^T\mathbf{x}^i+b=y_i$.

The optimum bias can be computed using this. In practice, it is better to average the values obtained by considering the set of all support vectors, according to

$$b=\frac{1}{\#SV}\sum_{i\in SV}\left(y_i-\sum_{k=1}^{m}\alpha_k y_k(\mathbf{x}^k)^T\mathbf{x}^i\right), \tag{8}$$

in which the expression (7) has been used.

The SVM formulation can be extended to non-separable classes. By introducing the slack variables ξ_k, the optimal class separation can be obtained from

$$\min\frac{1}{2}\mathbf{w}^T\mathbf{w}+C\sum_{k=1}^{m}\xi_k, \tag{9}$$

$$\begin{aligned}&\text{s.t. } y_k(\mathbf{w}^T\mathbf{x}^k+b)\ge 1-\xi_k,\\ &\xi_k\ge 0,\quad k=1,\cdots,m.\end{aligned} \tag{10}$$

In this case, the margin of separation is said to be soft. The constant $C > 0$ is user-defined and controls the tradeoff between maximization of the margin and minimization of classification errors on the training data set. The dual formulation of the QP is almost the same as (4)-(5). The only difference is in the bound constraints, which becomes

$$0\le\alpha_k\le C,\quad k=1,\cdots,m. \tag{11}$$

In this case, for the optimum Lagrange multipliers, we have $0<\alpha_k<C$ for the support vector; $\alpha_k=0$ for points correctly classified with $\xi_k=0$; and $\alpha_k=C$ for points with $\xi_k>0$. In the soft margin case, the relation (8) still holds, but the average is taken over all $\mathbf{x}^i$ such that $\alpha_i>0$.

Finally, the threshold b may be chosen *a priori*. In this case, the SVM can be trained by finding the minimum of

$$J(\boldsymbol{\alpha})=-\sum_{k-1}^{m}(1-b)\alpha_k+\frac{1}{2}\sum_{k=1}^{m}\sum_{j=1}^{m}\alpha_k\alpha_j y_k y_j(\mathbf{x}^k)^T\mathbf{x}^j, \tag{12}$$

subject to the bound constraints

$$0\le\alpha_k\le C,\quad k=1,\cdots,m.$$

With respect to the general formulation, the equality constraint (5) disappears, and it is easier to find the solution. From the optimum Lagrange multipliers, one obtains the weight vector using (7).

The SVMs can be applied to regression problems by the introduction of an alternative loss function [22], [23]. The basic idea in SVR is the mapping of the input data x onto a higher dimensional feature space via nonlinear mapping Φ. Then, a linear regression problem is obtained and solved in this feature space.

Consider the problem of approximating the set of data,

$$D=\left\{(x^1,y^1),\cdots,(x^l,y^l)\right\},\ x\in\mathbf{R}^n,y\in\mathbf{R}, \tag{13}$$

with the linear function

$$f(x)=\langle w,x\rangle+b. \tag{14}$$

The optimal regression function is given by the minimum of the functional:

$$\Phi(w,\xi)=\frac{1}{2}\|\mathbf{w}\|^2+C\sum_i(\xi_i^-+\xi_i^+), \tag{15}$$

where C is a pre-specified value, and ξ_i^- and ξ_i^+ are slack variables representing the upper and lower constraints, respectively, on the outputs of the system.

Using a quadratic loss function

$$L_{\text{quad}}(f(\mathbf{x})-y)=(f(\mathbf{x})-y)^2, \tag{16}$$

the solution is given by

$$\begin{aligned}\max_{\alpha,\alpha^*}\mathbf{w}(\alpha,\alpha^*)=\max_{\alpha,\alpha^*}&-\frac{1}{2}\sum_{i=1}^{l}\sum_{j=1}^{l}(\alpha_i-\alpha_i^*)(\alpha_j-\alpha_j^*)\langle\mathbf{x}_i,\mathbf{x}_j\rangle\\&+\sum_{i=1}^{l}(\alpha_i-\alpha_i^*)y_i-\frac{1}{2C}\sum_{i=1}^{l}(\alpha_i^2+(\alpha_i^*)^2).\end{aligned} \tag{17}$$

The corresponding optimization can be simplified by exploiting the Karush-Kuhn-Tuchker (KKT) conditions $\bar{\alpha}_i\bar{\alpha}_i^*=0, i=1,\cdots,l$, and noting that these imply $\beta_i^*=|\beta_i|$. The resultant optimization problems is given by

$$\min_{\beta}\frac{1}{2}\sum_{i=1}^{l}\sum_{j=1}^{l}\beta_i\beta_j\langle\mathbf{x}_i,\mathbf{x}_j\rangle-\sum_{i=1}^{l}\beta_i y_i+\frac{1}{2C}\sum_{i=1}^{l}\beta_i^2, \tag{18}$$

with the constraints $\sum_{i=1}^{l}\beta_i=0$.

The regression function is given by (14), where

$$\bar{\mathbf{w}}=\sum_{i=1}^{l}\beta_i\mathbf{x}_i,$$

$$\bar{b}=-\frac{1}{2}\langle\bar{\mathbf{w}},(\mathbf{x}_r+\mathbf{x}_s)\rangle,$$

and $\mathbf{x}_r$, $\mathbf{x}_s$ are any support vectors from each class satisfying $\alpha_r,\alpha_s>0, y_r=-1, y_s=1$.

Where a linear boundary is inappropriate, the SVM can map the input vector x onto a high dimensional feature space. By choosing a nonlinear mapping *a priori*, the SVM constructs an optimal separating hyperplane in this higher dimensional space. Kernel function can be used to perform the nonlinear mapping onto the feature space. The regression function is replaced by the kernel function

$$f(\mathbf{x})\sum_{SVs}(\bar{\alpha}_i-\bar{\alpha}_i^*)K(\mathbf{x}_i,\mathbf{x})+\bar{b}.$$

Table 2. Kernel functions and corresponding accuracy of humanoid robot on a flat ground.

Kernel type	*x*-coordinate	*y*-coordinate
Linear	47.184	60.704
Polynomial	9.695	18.568
RBF	2.524	2.721

Different kernels generate inner products to construct machines with different types of nonlinear decision surfaces in the input space. In this paper, the following three kinds of kernel functions are employed:

$$\begin{aligned} &\text{linear:} && K(x,y) = x^T y, \\ &\text{polynomial:} && K(x,y) = (xy+1)^d, \\ &\text{RBF:} && K(x,y) = \exp(-\|x-y\|^2 2\delta^2). \end{aligned} \tag{19}$$

An advantage of a linear kernel is that no parameter has to be tuned except for the constant C. Here, the constant C is set at 1,000. Moreover, the degree of the polynomial and the width of the RBF are set to 2.

IV. Walking Pattern Identification

Using three types of kernel functions (linear, polynomial, and RBF) for SVR, approximated models are constructed and their results are compared. The accuracy of each result is quantified in terms of the mean squared error (MSE) values. The SVR uses ideal ZMP data to model the ZMP trajectory of the humanoid robot as previously described. In Table 2, MSE values corresponding to the three types of kernel functions are listed for the humanoid robot walking on a flat surface. The results can be compared with respect to various kernel functions.

As seen in Table 2, the linear and polynomial kernels provide worse results than the RBF kernel. In addition, the polynomial kernel takes a longer time in the procedure. The generated ZMP positions from the RBF kernel and their errors between the actual data and the generated data are shown in Fig 10. The figure also presents the corresponding ZMP trajectories that are generated from the RBF kernel and their error distribution, which contains the information for the state and range of each position error. The figure shows that the generated ZMP is very similar to the ideal ZMP trajectory of the biped humanoid robot.

Another series of comprehensive experiments was conducted, and the results are also summarized. Other results using SVR for the humanoid robot walking on a sloped floor are shown in Table 3. The SVR with the RBF kernel achieved the best results among the kernel functions. Similarly, for the

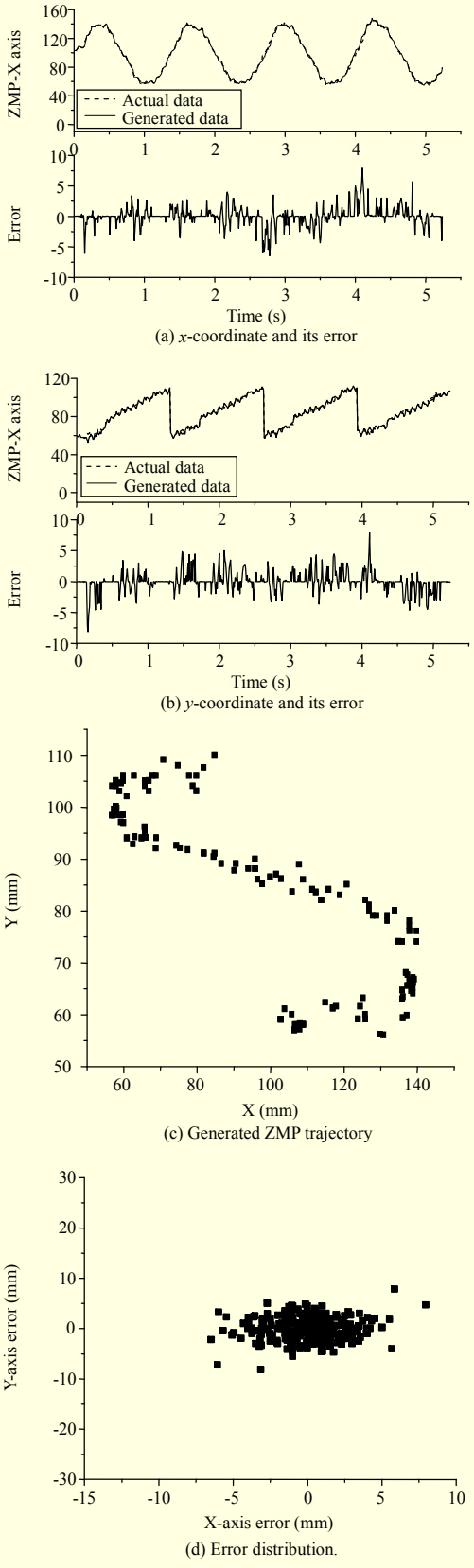

Fig. 10. Generated ZMP positions and corresponding trajectory of biped humanoid robot.

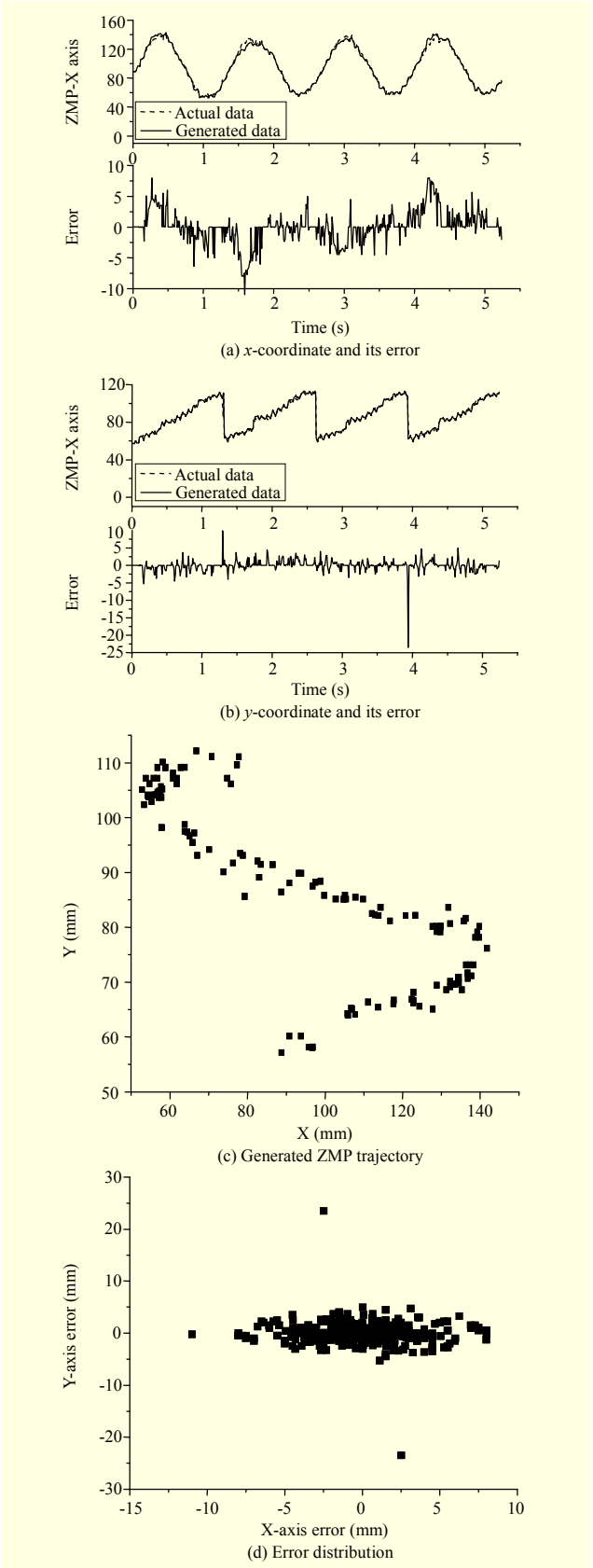

Fig. 11. Generated ZMP positions and corresponding trajectory of biped humanoid robot on a surface inclined 10°.

Table 3. Kernel functions and corresponding accuracy of humanoid robot on a surface inclined 10°.

Kernel type	*x*-coordinate	*y*-coordinate
Linear	48.28	58.648
Polynomial	15.313	18.287
RBF	6.938	3.732

Table 4. Results from comparison of SVR with other methods.

Methods and structure parameters		X:Y axis
Flat	Linear regression model: $f_1(\mathbf{x})$	7.780 : 13.558
	Fuzzy system: 1,024 fuzzy rules	4.164 : 4.763
	Fuzzy system: 256 fuzzy rules	4.249 : 4.59
	SVR model: 524 support vectors	2.524 : 2.721
Slope	Linear regression model: $f_2(\mathbf{x})$	13.661 : 15.560
	Fuzzy system: 1,024 fuzzy rules	8.552 : 5.011
	Fuzzy system: 256 fuzzy rules	8.862 : 6.443
	SVR model: 524 support vectors	6.938 : 3.732

two types of walking surfaces, namely, flat and inclined, the RBF kernel function produced the best results. Therefore, we concluded that the SVR with RBF structures as defined for the two types of walking surface is most likely to yield the best model for stable walking of a humanoid robot.

Figure 11 shows the generated ZMP positions and their trajectory determined using SVR with the RBF kernel. The figure presents the positions and the corresponding errors. The ZMP trajectory corresponding to the generated positions and their error distributions is also shown. To show the excellent overall performance which results from the SVR approach, it is compared with other methods. Table 4 compares the performance of the SVR with that of other techniques that have been proposed in the literature [17], [18]. The linear regression model used in [18] for flat and sloped surfaces is given in (20). Its parameters for a flat level surface and an upward slope are shown in Table 5. Using 10 inputs and 66 parameters, the linear model was formed. As a fuzzy system, 256 fuzzy rules or 1,024 fuzzy rules were considered, and their different results are compared in Table 4. SVR models using three kinds of kernel functions, namely, linear, polynomial, and RBF, and 524 support vectors are utilized and considered. The corresponding MSE values are shown in Tables 3 and 4. The results were compared on the basis of the same performance index for the actual ZMP trajectory. The SVR model outperformed the other models; therefore, the SVR can be effectively used to model and control a complex human-like walking mechanism.

$$f(\mathbf{x}) = c_0 + c_1x_1 + c_2x_2 + c_3x_3 + c_4x_4 + c_5x_5 + c_6x_6 + c_7x_7 + c_8x_8 + c_9x_9 + c_{10}x_{10} + c_{11}x_1^2 + c_{12}x_2^2 + c_{13}x_3^2 + c_{14}x_4^2 + c_{15}x_5^2 + c_{16}x_6^2 + c_{17}x_7^2 + c_{18}x_8^2 + c_{19}x_9^2 + c_{20}x_{10}^2 + c_{21}x_1x_2 + c_{22}x_1x_3 + c_{23}x_1x_4 + c_{24}x_1x_5 + c_{25}x_1x_6 + c_{26}x_1x_7 + c_{27}x_1x_8 + c_{28}x_1x_9 + c_{29}x_1x_{10} + c_{30}x_2x_3 + c_{31}x_2x_4 + c_{32}x_2x_5 + c_{33}x_2x_6 + c_{34}x_2x_7 + c_{35}x_2x_8 + c_{36}x_2x_9 + c_{37}x_2x_{10} + c_{38}x_3x_4 + c_{39}x_3x_5 + c_{40}x_3x_6 + c_{41}x_3x_7 + c_{42}x_3x_8 + c_{43}x_3x_9 + c_{44}x_3x_{10} + c_{45}x_4x_5 + c_{46}x_4x_6 + c_{47}x_4x_7 + c_{48}x_4x_8 + c_{49}x_4x_9 + c_{50}x_4x_{10} + c_{51}x_5x_6 + c_{52}x_5x_7 + c_{53}x_5x_8 + c_{54}x_5x_9 + c_{55}x_5x_{10} + c_{56}x_6x_7 + c_{57}x_6x_8 + c_{58}x_6x_9 + c_{59}x_6x_{10} + c_{60}x_7x_8 + c_{61}x_7x_9 + c_{62}x_7x_{10} + +c_{63}x_8x_9 + c_{64}x_8x_{10} + c_{65}x_9x_{10} \quad (20)$$

Table 5. Parameters of linear regression model in Table 4.

Regression parameters of $f_1(\mathbf{x})$	
X-axis	Y-axis
108.4851, 10.3680, 1.1915, 0.3362, 1.7275, 4.8259, -15.8207, 9.3517, 12.1248, 13.4999, -5.1264, -1.4948, 0.0266, 0.0248, 0.0087, 33.6153, 0.3332, 0.0135, -0.0065, 0.0056, 35.4128, 0.1214, 0.1621, -0.5563, 0.1647, 1.4391, 2.2490, 1.5958, 0.7898, -1.5917, 0.0859, 0.1228, -2.2760, 0.0914, -0.0063, 0.0771, 0.1808, 2.4820, 0.0346, 0.3618, -0.3191, 0.1166, 0.1081, 0.1438, -0.3584, 2.2013, -0.1043, 0.2550, 0.0290, -0.2450, -2.7943, -1.6056, -0.0698, -2.1067, -3.7469, -68.6840, -1.7849, -1.3543, -0.5701, 3.6694, -0.0141, 0.0227, 0.5020, 0.0262, 2.4449, 4.0112	52.0680, -17.7514, -1.0354, 0.0839, -4.2881, 8.7571, 25.0461, -19.0592, -18.5020, -17.2340, -5.1585, 1.4533, -0.0253, -0.0380, -0.0215, 7.9889, -0.1767, -0.1888, 0.0389, 0.2932, 8.2107, -0.4401, -0.4358, 0.4247, -2.5863, -1.4285, -2.1032, -1.4435, -0.4710, 3.8090, -0.0496, -0.1249, 2.5672, 0.2856, -0.1162, -0.2939, -0.4875, -2.6680, -0.1146, 2.4848, 0.5023, 0.2796, 0.1778, 0.1036, -2.5564, 1.9734, -0.0500, 0.7608, 0.8599, 1.2586, -1.6399, 1.9891, 2.7305, 1.7249, 0.7790, -16.4875, 1.2562, 0.6322, -0.4848, -3.6612, -0.1458, 0.0667, -3.4481, 0.3277, -2.5003, -1.7484
Regression parameters of $f_2(\mathbf{x})$	
X-axis	Y-axis
31.5798, -8.8204, -0.4683, -0.2844, 0.8990, -2.9537, 6.7073, -10.2923, -4.4366, 0.6653, 5.3366, -0.2683, 0.0438, 0.0117, -0.0113, -1.9453, 0.1702, -0.1431, -0.0489, 0.1250, -1.4257, -0.5467, -0.5040, -0.6150, 1.4378, 0.4543, -0.4429, -0.3305, 0.0649, -1.5312, 0.0894, 0.0735, -1.4971, 0.7066, 0.1695, 0.1273, 0.1049, 1.6218, -0.0213, -0.7997, 0.4173, 0.3769, 0.2642, 0.1013, 0.7901, -0.0711, 0.1841, 0.6104, 0.3447, -0.0077, -0.3119, -1.5248, -1.6166, -0.8470, -0.3548, 3.6680, 0.4649, 0.3974, 0.3150, 2.2714, -0.1978, 0.0073, 1.6824, 0.1023, 1.0467, 0.7198	3.9218, -41.2045, -5.1537, 3.9998, 3.9269, 14.8381, 24.4839, -23.8715, -19.9409, -16.4117, -34.1381, 0.0429, 0.0313, 0.0307, 0.0018, 0.1937, -0.5284, -0.2007, 0.0116, 0.0721, 0.2094, -0.8562, 0.0153, 0.8259, -0.5773, 0.4057, -4.8924, -3.6009, -1.7948, 0.8884, 0.0414, -0.0357, 0.9235, 0.2915, -0.5816, -0.7679, -0.9975, -1.3372, 0.0274, 0.4515, -0.1458, -0.4310, -0.4380, -0.6066, -0.6480, 0.0207, -0.5257, -0.4860, -0.2706, -0.0880, 0.2174, 0.3350, 2.5836, 2.0706, 1.2253, -0.4741, 3.1642, 2.2698, 1.1578, -0.7969, -0.1573, -0.1707, -4.0365, 0.0476, -3.1981, -1.6756

V. Conclusion and Future Research

Stable walking pattern identification (analysis) using SVR by considering the ZMP trajectory of a practical biped walking robot was investigated in this paper. The focus of the paper was ZMP walking pattern identification of a practical humanoid robot using SVR for stable walking. The trajectory of the ZMP is an important criterion for the stability of walking robots even though it is difficult to generate stable and natural walking motion for a robot.

In this paper, two types of natural motions of humanoid robot were employed for reference and SVR was applied to analyze stable walking motions by considering these actual motions. It was found that the SVR approach performed well and SVR with the RBF kernel function generated the best results.

When a humanoid robot walks on a flat surface, the ZMP of the robot is generally included in the convex hull of the foot-supporting area. However, the robot may suddenly become unstable and begin to tip over when there are unexpected sudden events. In that case, the ZMP becomes uncontrollable, since the contact force between the ground and the feet cannot provide the necessary recovery moment to control the ZMP. Therefore, there is still much work to be done. Some important future works will concern control issues and time consumption. Recently intelligent soft computing algorithms, particularly using fuzzy systems, neural networks (NNs), and genetic algorithms, have been developed. In particular, NNs do not require prior knowledge about the target system to be controlled or handled and will be efficient in learning nonlinear control models from input and output data obtained from real target systems. They may be incorporated in controlling the ZMP of a humanoid robot to achieve walking stability. In future works, we will work to design humanoid robot systems and intelligent computing algorithms without heavy cost and time consumption.

References

[1] Y. Guan et al., "Stepping Over Obstacles With Humanoid Robots," *IEEE Trans. Robotics*, vol. 22, no. 5, 2006, pp. 958-973.

[2] E. Neo et al., "A Switching Command-Based Whole-Body Operation Method for Humanoid Robots," *IEEE/ASME Trans. Mechatronics*, vol. 10, no. 5, 2005, pp. 546-559.

[3] M. Hirose, Y. Haikawa, and T. Takenaka, "Introduction of Honda Humanoid Robots Development," *Proc. Adv. Sci. Ins.*, no. 16, 2001, pp. 1-8.

[4] F. Yamasaki et al., "PINO: The Humanoid that Walks," *Proc. IEEE-RAS Int. Conf. Humanoid Robots*, 2000.

[5] M. Gienger, K. Loffler, and F. Pfeiffer, "Towards the Design of a Biped Jogging Robot," *Proc. IEEE Int. Conf. Robotics Automation*, vol. 4, 2001, pp. 4140-4145.

[6] C.L. Vaughan, "Theories of Bipedal Walking: An Odyssey," *J. Biomechanics*, vol. 36, 2003, pp. 513-523.

[7] T. Reil and C. Massey, "Biologically Inspired Control of Physically Simulated Bipeds," *Theory in Biosci.*, vol. 120, 2001, pp. 327-339.

[8] N. Ogihara and N. Yamazaki, "Generation of Human Bipedal Locomotion by a Bio-mimetric Neuro-musculo-skeletal Model," *Biol. Cybern.*, vol. 84, 2001, pp. 1-11.

[9] J. Vermeulen et al., "Trajectory Planning for the Walking Biped 'Lucy'," *Int. J. Robotics Research*, vol. 25, no. 9, 2006, pp. 867-887.

[10] Y. Hasegawa, T. Arakawa, and T. Fukuda, "Trajectory Generation for Biped Locomotion Robot," *Mechatronics*, vol. 10, 2000, pp. 67-89.

[11] M. Vukobratovic et al., *Biped Locomotion*, New York, NY: Springer Verlag, 1990.

[12] C.L. Shih et al., "Trajectory Synthesis and Physical Admissibility for a Biped Robot During the Single Support Phase," *Proc. IEEE Int. Conf. Robotics and Automation*, vol. 3, 1990, pp. 1646-1652.

[13] A. Dasgupta and Y. Nakamura, "Making Feasible Walking Motion of Humanoid Robots from Human Motion Capture Data," *Proc. IEEE Int. Conf. Robotics and Automation*, vol. 2, 1999, pp. 1044-1049.

[14] A. Takanish et al., "The Realization of Dynamic Walking Robot WL-10RD," *Proc. Int. Conf. Advanced Robotics*, 1985, pp. 459-466.

[15] K. Hirai et al., "The Development of Honda Humanoid Robot," *Proc. IEEE Int. Conf. Robotics and Automation*, vol. 2, 1998, pp. 1321-1326.

[16] Q. Huang et al., "Planning Walking Patterns for a Biped Robot," *IEEE Trans. Robotics Automation*, vol. 17, no. 3, 2001, pp. 280-288.

[17] D. Kim et al., "Fuzzy Modeling of Zero Moment Point Trajectory for a Biped Walking Robot," *Lect. Notes Artif. Int.,* vol. 3214, 2005, pp. 716-722.

[18] D. Kim, S.J. Seo, and G.T. Park, "Zero-Moment Point Trajectory Modeling of a Biped Walking Robot Using an Adaptive Neuro-fuzzy Systems," *IEE Proc. Control Theory Appl.*, vol. 152, 2005, pp. 411-426.

[19] D. Kim et al., "Evolutionary Design of Sugeno-Type Fuzzy System for Humanoid Robot Modeling," *Int. J. Syst. Sci.*, Accepted for publication.

[20] M. Vukobratovic and B. Brovac, "Zero-Moment Point-Thirty Five Years of Its Life," *Int. J. Humanoid Robotics*, vol. 1, 2004, pp. 157-173.

[21] V. Vapnik, *The Nature of Statistical Learning Theory*, New York: John Wiley, 1995.

[22] S. Gunn, *Support Vector Machines for Classification and Regression*, *ISIS Technical Report*, Image Speech & Intelligent Systems Group, University of Southampton, England, 1998.

[23] W. Wang and Z. Xu, "A Heuristic Training for Support Vector Regression," *Neurocomputing*, vol. 61, 2004, pp. 259-275.

[24] D. Casali et al., "Associative Memory Design Using Support Vector Machines," *IEEE Trans. Neural Networks*, vol. 17, no. 5, 2006, pp. 1165-1174.

[25] S. Haykin, *Neural Networks: A comprehensive Foundation*, 2nd ed., Upper Saddle River, NJ: Prentice-Hall, 1999.

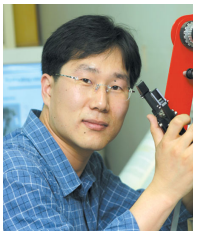

Dong Won Kim received the PhD in electrical engineering from Korea University, Seoul, Korea, in 2007. He was a post-doctoral research scholar with Berkeley Initiative in Soft Computing (BISC), University of California, Berkeley, in 2008 and Advanced Highway Maintenance and Construction Technology Research Center (AHMCT), University of California, Davis, in 2009. He is now a professor with the Department of Digital Electronics of Inha Technical College, Incheon, Korea. His research focuses on the intelligent humanoid robot, autonomous multi-mobile robot navigation, and robot intelligence based on the neuro-fuzzy system. He is an editorial board member of *International Journal of Control and Automation*, and an editor of the *Journal of Convergence Information Technology* and the *International Journal of Advancements in Computing Technology*. He is a program committee member and associate editor of several international conferences, and a reviewer of *IEEE Trans. Systems, Man, and Cybernetics*, and the *International Journal of Systems Science*. He received the Best Paper Award from the international conference on Knowledge-Based & Intelligent Information & Engineering Systems, the Best Student Paper Competition Finalist Award at the IEEE international conference on SMC in 2003, the Prize from Seoam Scholarship Foundation in 2002, and he was the prize winner of the Student Paper Contest from IEEE Korea Council in 2000.

Sam-Jun Seo received the BS, MS, and PhD degrees in electrical engineering from Korea University, Seoul, Korea, in 1989, 1991, and 1996, respectively. He joined Anyang University, Gyeonggido, Korea, in 1997, and is currently an associate professor with the Department of Electrical and Electronic Engineering. His research interests include intelligent control, fuzzy systems, neural networks, tele-operating systems, and intelligent robots.

Clarence W. de Silva earned the PhD degrees from Massachusetts Institute of Technology (1978); and University of Cambridge, UK (1998); and an honorary .Eng degree from University of Waterloo, Canada (2008). He is a professor of mechanical engineering with the University of British Columbia, Vancouver, Canada, and has held the NSERC-BC Packers Chair in Industrial Automation since 1988. He occupies the Tier 1 Canada Research Chair in Mechatronics & Industrial Automation. Dr. de Silva is a Fellow of the Royal Society of Canada, IEEE, ASME, and the Canadian Academy of Engineering. He is also a registered Professional Engineer of BC. He has authored 19 books, 185 journal articles, including the most recent books published by Taylor & Francis/CRC: *Modeling and Control of Engineering Systems* (2009), *Sensors and Actuators—Control System Instrumentation* (2007), *VIBRATION—Fundamentals and Practice, 2nd Ed.* (2007), and *Mechatronics—An Integrated Approach* (2005). He has served on editorial boards of 12 international journals including IEEE and ASME Transactions, and as Editor-in-Chief of the *International Journal, Control and Intelligent Systems*.

Gwi-Tae Park received his BS, MS, and PhD degrees in electrical engineering from Korea University, Seoul, Korea, in 1975, 1977, and 1981, respectively. He was a technical staff member with the Korea Nuclear Power Laboratory and an electrical engineering faculty member at Kwangwoon University, in 1975 and 1978, respectively. He joined Korea University in 1981 where he is currently a professor with the School of Electrical Engineering. He was a visiting professor with the University of Illinois in 1984. He is a fellow of the Korean Institute of Electrical Engineers (KIEE), the Institute of Control, Automation, and System Engineers Korea (ICASE), and advisor of the Korea Robotic Society. He is also a member of the Institute of Electrical and Electronics Engineers (IEEE) and the Korea Fuzzy Logic and Intelligent Systems Society (KFIS).